Deep-Sea Research Part II 164 (2019) 14–24

Contents lists available at ScienceDirect

Deep-Sea Research Part II

journal homepage: www.elsevier.com/locate/dsr2

Decadal variations of circulation in the Central Mediterranean and its interactions with mesoscale gyres

M. Menna[a,*], N.C. Reyes Suarez[a,b], G. Civitarese[a], M. Gačić[a], A. Rubino[c], P.-M. Poulain[a,d]

[a] Istituto Nazionale di Oceanografia e di Geofisica Sperimentale – OGS, Sgonico, TS, Italy
[b] Abdus Salam International Center for Theoretical Physics - ICTP, Trieste, Italy
[c] Università degli Studi di Venezia Ca' Foscari, Venezia, Italy
[d] Centre for Marine Research and Experimentation – CMRE, La Spezia, Italy

ARTICLE INFO

Keywords:
Northern Ionian Gyre reversals
Decadal variability
Interannual variability
Messina Rise Vortex
Pelops Gyre

ABSTRACT

The most prominent oceanographic features in the Central Mediterranean are decadal reversals of the Northern Ionian Gyre (NIG), interpreted in terms of internal processes. Altimetry data, drifter data and model surface salinity products are used in this paper to define some specific features of the circulation related to the anticyclonic or cyclonic NIG modes. Results not only highlight different shapes and intensities of the Mid-Ionian Jet and northern Ionian meander among the two circulation mode, but emphasize distinct behaviour within the same mode, imputable to the variability of the mesoscale quasi-permanent features. The wind-driven Messina Rise Vortex, on the western side of the northern Ionian, and the Pelops Gyre, on the eastern side of the northern Ionian, show different behaviour during the first (1993–1996) and the second (2006–2010) anticyclonic periods, related to the cyclonic activity along the dense water pathway. When the dense water was of Aegean origin (1993–1996; "Aegean" anticyclone), the cyclonic mesoscale activity on the eastern flank of the Ionian overwhelmed the anticyclonic wind forcing, and led to the disappearance of the Pelops Gyre. When the dense water was of Adriatic origin (2006–2010; "Adriatic" anticyclone), the strengthening of cyclonic mesoscale activity on the western flank of the Ionian caused the shape change of the Messina Rise Vortex, favouring its longitudinal extension. The zonally-elongated Messina Rise Vortex reduced the inflow of Atlantic Water in the northern Ionian, and induced a strengthening of the eastward flowing Mid-Ionian Jet in the southern Ionian and Cretan Passage. From these results, it emerges that the interannual variability of the wind-driven quasi-permanent mesoscale gyres in the Ionian is influenced by internal forcing (location of the deep water formation site – Aegean or Adriatic Sea), in turn related to the major local climatic shift occurred in the last decades (the Eastern Mediterranean Transient). We show that the interplay between decadal and interannual variability, or rather between basin-wide and mesoscale circulation, affected the intrinsic characteristics of the NIG reversals.

1. Introduction

The Central Mediterranean Sea (CMS), defined in this paper as the area between 29.2° – 41°N and 12° – 26.5°E (see Fig. 1 for geographical reference), includes the Sicily Channel (SC), the Ionian Sea (IS) and the Cretan Passage (CP). The first attempt to define the main circulation and water masses pathways in the CMS dates back to 1990's, when Malanotte-Rizzoli et al. (1997) made a schematic map, based on hydrographic data collected in 1986–1987 (POEM-Phase I experiment), which already identified the key structures of the CMS dynamics. The authors described the inflow of the Atlantic Water (AW) in the SC through the Atlantic Ionian Stream (AIS), jet which enters the IS and bifurcates in two main branches: one branch turns southward, whereas the second branch advects the AW toward the northern Ionian, then turns southward to cross the entire IS meridionally and finally veers to the east and enters the CP. This meander of AW, that moves into the Ionian and feed the eastward flow in the Cretan Passage, was subsequently defined as Mid-Ionian Jet (MIJ; Robinson et al., 2001).

A few years later, Demirov and Pinardi (2002) detected two different behaviours in the IS circulation before and after 1987, characterised by an inversion of the surface circulation from cyclonic to anticyclonic in 1987–1988. According to these authors, the change of the circulation modified the salinity of the Levantine Intermediate Water (LIW) transported toward the Aegean and the Adriatic Sea, influencing the deep water processes in these regions. An anomalous behaviour in the path of AIS toward the northern IS with respect to

* Corresponding author.
E-mail address: mmenna@inogs.it (M. Menna).

https://doi.org/10.1016/j.dsr2.2019.02.004

Available online 12 February 2019

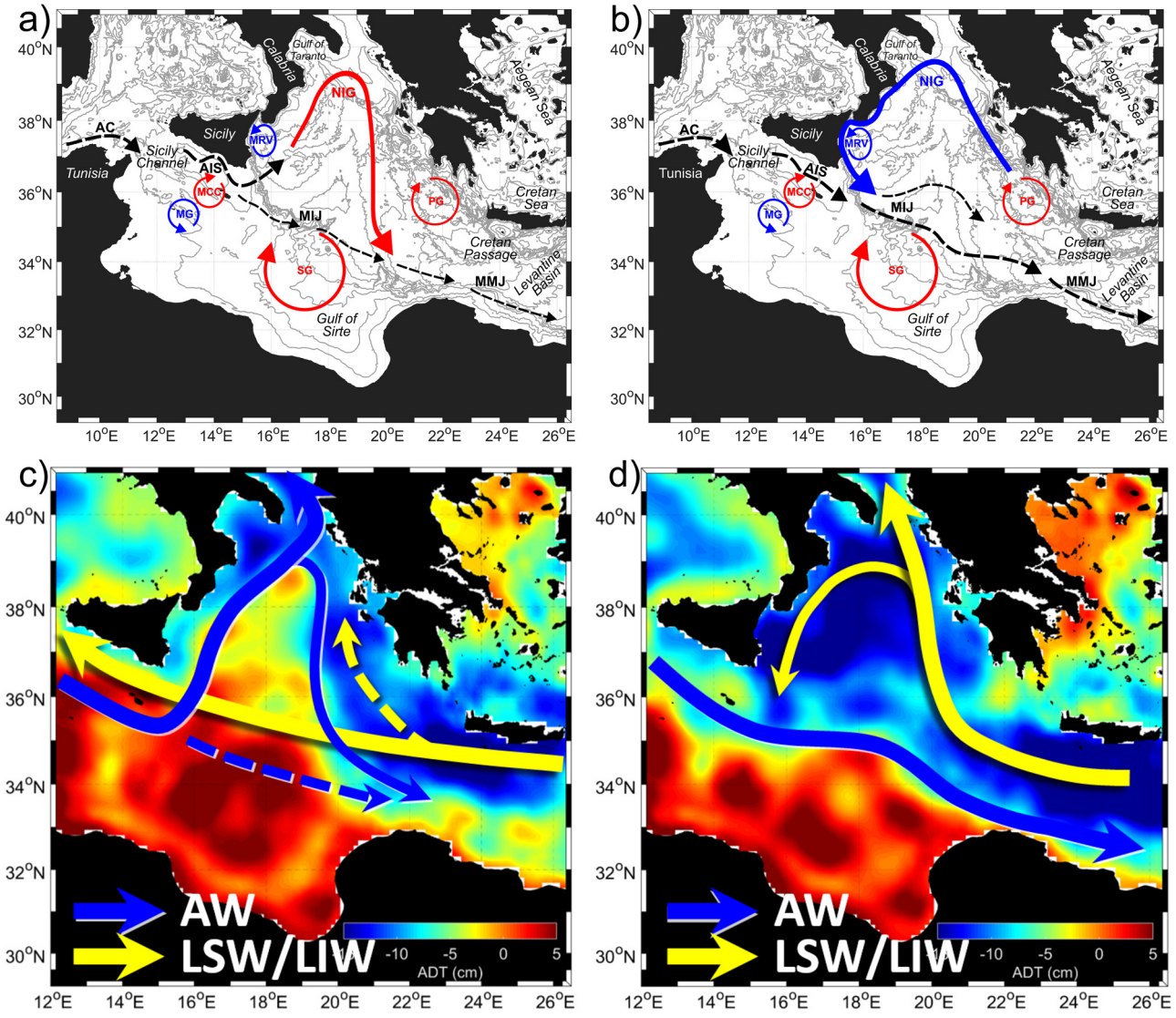

Fig. 1. Geography and bathymetry of the CMS superimposed with a schematic representation of the main surface currents (black arrows), anticyclonic (red arrows) and cyclonic (blue arrows) features during the a) anticyclonic and b) cyclonic modes of NIG; summary of the water masses distribution during the c) anticyclonic and d) cyclonic NIG (the background maps are ADT annual average in 1996 and 2003, respectively). Acronyms are listed in Table 1.

those described in 1986–1987 by Malanotte-Rizzoli et al. (1997), was already observed by Brandt et al. (1999) investigating the tidally-induced internal dynamics in the Strait of Messina during autumn 1995. In this new perspective, the situation described by Malanotte-Rizzoli et al. (1997) corresponded to the northern Ionian anticyclonic mode of circulation, and the behaviour of the currents and water masses during the cyclonic mode was still to be discovered. In the following years, the interannual variability of the CMS was studied in order to better understand the impact of these reversals on the circulation structures, on the biogeochemistry and biology of the Eastern Mediterranean and on the thermohaline properties of the whole Mediterranean Sea.

The discovery of two different circulation patterns in the northern Ionian also led to an update of the nomenclature of circulation structures in the basin. In detail the MIJ, defined in Robinson et al. (2001) as the meridional current which crosses the northern-Ionian in the north-south direction before creating the Mid-Mediterranean Jet (MMJ), was successively considered as a quasi-zonal, south-eastward extension of the AIS which flows into the IS (south of 36°N) from the west to east, connecting the SC with the CP (Gačić et al., 2011, 2014; Bessieres et al., 2013). The northern Ionian meander was instead defined as northern Ionian Gyre (NIG; Civitarese et al., 2010).

At present, it is known that the NIG is characterised by its quasi-decadal reversals which influences the strength of the MIJ and the properties of the Eastern Mediterranean thermohaline cell (Borzelli et al., 2009; Gačić et al., 2010; Civitarese et al., 2010). The NIG reversals are driven by internal processes (e.g. Pisacane et al., 2006; Borzelli et al., 2009; Gacic et al., 2010, 2011, 2014; Theocharis et al., 2014). The most accredited and cited process to explain such reversal is a feedback mechanism, named Adriatic-Ionian Bimodal Oscillation System (Gačić et al., 2010; Civitarese et al., 2010), driven by the difference in salinity (Figs. 1c, 1d) between the salty and warmer waters originating from the eastern Mediterranean (LIW- and Levantine Surface Water, – LSW), and the less saline AW entering from the SC (Gačić et al., 2011, 2014). Another possible mechanism proposed for explaining the NIG reversal is wind forcing (see Pinardi et al., 2015 and references therein).

During the anticyclonic phase of the NIG the AIS is deflected north-eastward (Fig. 1a) and brings AW toward the northern Ionian and eventually the Adriatic Sea (Fig. 1c); consequently, the flow of the AW in the Levantine basin is reduced (weakening of the MIJ) and the LSW becomes saltier (Gačić et al., 2014). The cyclonic phase of the NIG (Fig. 1b) partially blocks the inflow of the AIS toward the northern IS,

Table 1
List of acronyms used in this paper.

Geographical names and transects	
CMS	Central Mediterranean Sea
CP	Cretan Passage
IS	Ionian Sea
SC	Sicily Channel
Water masses	
AW	Atlantic Water
LIW	Levantine Intermediate Water
LSW	Levantine Surface Water
Currents	
AC	Algerian Current
AIS	Atlantic Ionian Sea
MIJ	Mid-Ionian Jet
MMJ	Mid-Mediterranean Jet
Gyres and eddies	
MCC	Maltese Channel Crest
MRV	Messina Rice Vortex
NIG	Northern Ionian Gyre
PG	Pelops Gyre
SG	Sirte Gyre
Climatic events	
EMT	Eastern Mediterranean Transect
Physical properties	
ADT	Absolute Dynamic Topography
AGV	Absolute Geostrophic Velocities
EKE	Eddy Kinetic Energy

therefore the AIS preferentially moves toward the mid IS (strengthening the MIJ) allowing the inflow of more saline water masses of the Levantine origin into the Adriatic basin (Fig. 1d). This situation due to the inflow of the salty Levantine waters facilitates the winter convection in the southern Adriatic area and leads to the formation of a denser Adriatic Dense Water. As a consequence of the high density water outflow from the Adriatic the lowering of the sea level along the flanks of the Ionian occurs and weakens the upper-layer cyclonic circulation (Gačić et al., 2010).

The NIG reversals influences also the depth of the nitracline (Civitarese et al., 2010) and the phytoplankton phenology (Lavigne et al., 2018) in the northern Ionian, and the biodiversity in the Adriatic Sea (Civitarese et al., 2010). Cyclonic (anticyclonic) circulation causes a downwelling (upwelling) of the nitracline (and of the nutrient maximum layer, too) along the borders of the NIG and a decrease (increase) in the nutrient content of the water flowing into the Adriatic across the sill (800 m deep) of the Otranto Strait (Civitarese et al., 2010). In addition, the advection of different water masses due to the NIG reversals can result in the entrance of allochtonous organisms in the Adriatic of either Atlantic/Western Mediterranean or Levantine/tropical origin (Civitarese et al., 2010). Associated with the NIG reversals, two different trophic regimes in the Ionian Sea occur (Lavigne et al., 2018): the anticyclonic NIG is characterised by an early winter bloom, whereas the cyclonic NIG supports a bloom onset in late winter and a chlorophyll peak in March.

The Levantine and Cretan seas salinities are out of phase with respect to the Ionian surface water salinity, and a dilution/salinification of the Levantine-Cretan waters during the cyclonic/anticyclonic NIG phases is observed (Gačić et al., 2011; Ozer et al., 2017). This relationship can be considered as a preconditioning for the Eastern Mediterranean Transient (EMT) -like phenomena (Artale et al., 2006; Pisacane et al., 2006; Gačić et al., 2011, Cardin et al., 2015). Salinity variations in the core of the LIW produced in the Levantine Basin are transferred through the SC and impact the Western Mediterranean. Gačić et al. (2013) showed that the travel time between the LIW formation site (Rhodes Gyre) and the SC is of about 11 yr, whereas the time lag between the SC and the Algero-Provençal basin is of about 4 yr. These authors concluded that the LIW salinity variations in the Eastern Mediterranean, in turn related to the NIG reversals, can be observed in the Western Mediterranean with a delay of about 15 yr, and could have created the conditions for the Western Mediterranean Transition, i.e. the sudden salinity and temperature increase in the deep layer of the Western Mediterranean basin occurring since 2004 (Schroeder et al., 2016).

Given the aforementioned considerations, it is clear that the NIG reversals has a significant impact, not only on the physical and chemical dynamics of the southern Adriatic and northern Ionian seas, but also on the Levantine Basin, the SC and Western Mediterranean. The goal of this study is to address the interaction between mesoscale and basin-scale circulations within the Ionian basin. More specifically, we consider two semi-permanent, wind-induced features: the Pelops Gyre (PG) and the Malta Rise Vortex (MRV). Altimetry, drifter data and model surface salinity products are used to describe common and peculiar characteristics of the NIG anticyclonic and cyclonic modes. Differences within the same circulation mode are identified and interpreted in terms of climatic events (like that induced by severe winter conditions in the Adriatic Sea) or sporadic interactions between the basin-wide circulation and mesoscale gyres in the IS. Also the mesoscale features are described in terms of their interannual variability and their dependence of the basin-scale deep circulation patterns.

2. Data and methods

The altimetry data used for this study were the gridded (1/8° Mercator projection grid), daily Absolute Dynamic Topography (ADT) and the corresponding Absolute Geostrophic Velocities (AGV) distributed by CMEMS (product user manual CMEMS-SL-QUID_008–032–051). Interannual means of the ADT and AGV were computed over the periods characterised by anticyclonic (1993–1996; 2006–2010) and cyclonic (1997–2005; 2011–2016) NIG circulation (Fig. 2, right panels).

The monthly means of the AGV were used to compute the interannual Eddy Kinetic Energy (EKE) field over the period for which altimetry data was available (25 years from 1993 to 2017; Fig. 6). In order to obtain an interannual mean excluding the seasonal variability of the signal, the monthly AGV climatology estimated over 25-years (i.e. $U_{Jan1993–2017}$; $U_{Feb1993–2017}$; $U_{Mar1993–2017,...}$; $V_{Jan1993–2017}$; $V_{Feb1993–2017}$; $V_{Mar1993–2017,}$ etc., where U and V are the zonal and meridional components of the AGV) was removed to each month (i.e. $U'_{Jan} = U_{Jan1993} - U_{Jan1993–2017}$; $V'_{Jan} = V_{Jan1993} - V_{Jan1993–2017}$) in every grid point. Finally, EKE values in each grid point were calculated from the AGV residuals (U' and V'):

$$EKE = \frac{1}{2}\langle U'^2 + V'^2 \rangle; \quad (1)$$

EKE field is used to locate the transects of Fig. 7i.e. where the currents inflow (outflow) in (from) the CMS or where they bifurcate.

Lagrangian data were taken from the MedSVP_db24 drifter dataset (Menna et al., 2018). Among the available products, we selected the database interpolated at 6 h and filtered at 36 h. More details about the drifter data and telemetry, editing and interpolation are available in Menna et al. (2017). Pseudo-Eulerian velocity statistics in bins of $0.5° \times 0.5°$ were computed over the NIG cyclonic/anticyclonic periods (Fig. 2; left panels). Due to their Lagrangian nature, drifters move with the currents and provide an accurate but irregular spatial and temporal sampling of near surface currents.

Salinity fields were derived from the surface (~ 1.5 m depth) MEDREA products (https://doi.org/10.25423/medsea_reanalysis_phys_006_004, distributed by CMEMS and available until 2016) using a variational data assimilation scheme for temperature/salinity vertical profiles and satellite Sea Level Anomaly along track data (Simoncelli et al., 2014). Mean maps of the surface salinity patterns were estimated over the NIG cyclonic/anticyclonic periods (Fig. 5).

The Cross-Calibrated, Multi-Platform (CCMP) V2.0 ocean surface wind velocity were downloaded from the NASA Physical Oceanography DAAC for the period July 1987 – May 2016 (Atlas et al., 2011). These

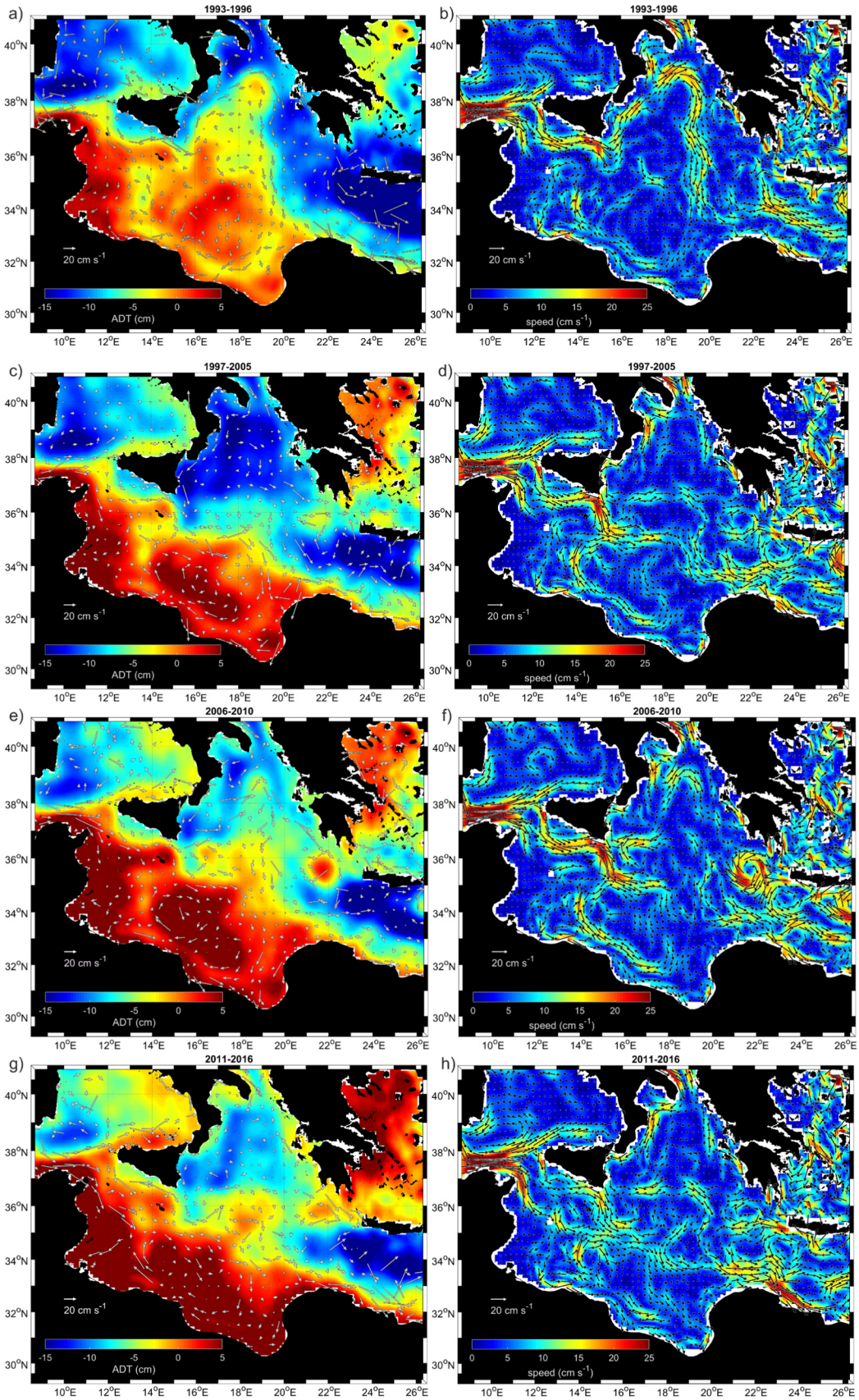

Fig. 2. Mean drifter currents in spatial bins of $0.5^{\circ} \times 0.5^{\circ}$ (arrows) superimposed on means map of ADT (colours) (left panels) and mean AGV (arrows) and relative speeds (colours) (right panels) in the CMS for the periods a) b) 1993–1996, c) d) 1997–2005 e) f) 2006–2010 and g) h) 2011–2016.

products were created using a variational analysis method to combine wind measurements derived from several satellite scatterometers and micro-wave radiometers. The CCMP six-hourly gridded analyses (level 3.0, first-look version 1.1, resolution of 25 km), were used to quantify the vertical component of the wind stress curl $[curl\ \tau]_z$ over the Sicily Channel:

$$[curl\tau]_z = \frac{\partial \tau_y}{\partial x} - \frac{\partial \tau_x}{\partial y};\ (\tau_y,\ \tau_x) = \rho C_D (u_w,\ v_w) U_{10} \tag{2}$$

where $(\tau_x \tau_y)$ are the wind stress components, ρ (1.22 kg/m^3) is the density of air, (u_w, v_w) and U_{10} are the components and the magnitude of the wind speed at 10 m, respectively, and C_D is the drag coefficient which has been obtained according to Yelland and Taylor (1996) and was already used in the Mediterranean Sea by Shabrang et al. (2016):

$$\begin{aligned} C_D &= 10^{-3} && |U_{10}| \le 3\tfrac{m}{s} \\ C_D &= \left(0.29 + \tfrac{3.1}{U_{10}} + \tfrac{7.7}{U_{10}^2}\right) \times 10^{-3} && 3\tfrac{m}{s} \le |U_{10}| \le 6\tfrac{m}{s} \\ C_D &= (0.6 + 0.07 U_{10}) \times 10^{-3} && 6\tfrac{m}{s} \le |U_{10}| \le 26\tfrac{m}{s} \end{aligned} \tag{3}$$

Wind stress vorticity fields were used to speculate on the link between the wind variations and the interannual variability of mesoscale and sub-basin scale structures.

Monthly means of the AGV field were used to estimate the relative vorticity (ζ), defined as the vertical component of the velocity field curl

$$\zeta = \frac{\partial V}{\partial x} - \frac{\partial U}{\partial y}; \tag{4}$$

where U and V are the velocity components of the AGV. The resulting geostrophic currents vorticity fields and the wind stress vorticity were spatially averaged in the region of PG (35–36.5°N; 20–22.5°E) and filtered (13-month moving average) in order to remove the seasonal and intra-annual variations (Fig. 4).

The time series of the monthly geostrophic velocity components perpendicular to the transects depicted in Fig. 6 are depicted in Fig. 7. Transect locations were chosen in order to intercept both the main pathways of surface currents in the CMS and the regions with the larger values of the interannual EKE field.

3. Results and discussion

The reversals of the NIG circulation are documented from altimetry and drifter data since 1993, with the occurrence of two anticyclonic (1993–1996 and 2006–2010) and two cyclonic (1997–2005 and 2011–2016) modes (Fig. 2). The anticyclonic mode of 1993–1996, actually started before the temporal coverage of altimetry data (in 1987–1988 according to Demirov and Pinardi, 2002). In addition, a recent reversal of the surface circulation of the NIG from cyclonic to anticyclonic was observed in the second half of 2017 (Notarstefano et al., 2019, section 4.5 in von Schuckmann et al., 2019).

The inversion of 2006 to anticyclonic mode was supported by altimetry data (Gačić et al., 2014) and ocean state indices (Bessieres et al., 2013; Reale et al., 2017), but it was not sustained by the MEDREA reanalysis products that documented only a weakening of the cyclonic circulation in the period 2006–2016 (Pinardi et al., 2015; Simoncelli et al., 2018, section 3.4 in von Schuckmann et al., 2017). In order to dispel these doubts and to confirm the circulation inversion noticed from the satellite data, the altimetry ADT fields were qualitatively compared with velocity measurements derived from drifters (Fig. 2; left panels). The bin size selected for the Lagrangian statistics (0.5° × 0.5°) was a compromise to resolve the basin and sub-basin scale circulation and, at the same time, to obtain robust statistics in each bin; unfortunately, mesoscale and sub-mesoscale velocities were not resolved.

Left panels of Fig. 2 show the mean drifter currents superimposed on the mean ADT fields during the periods characterised by anticyclonic/cyclonic modes. The two datasets fit rather well, confirming the alternance of the two circulation modes, the occurrence of the anticyclonic mode in 2006–2010, and the peculiar shapes of the basin and sub-basin scale circulation features related to the NIG. The anticyclonic mode in 2006–2010 is indirectly confirmed also from the results of Ozer et al. (2017) in the Levantine Basin. These authors observed two salinity maxima of the LSW and LIW in 1991 and 2008, related to periods of anticyclonic circulation in the northern Ionian (1987–1996 and 2006–2010, respectively).

The right panels of Fig. 2 depict the mean AGV derived from altimetry data (arrows) superimposed on the corresponding speed (colours). West of 15°E and south of 35°N, the pattern of the main currents was not influenced by the NIG circulation mode: the Algerian Current (AC) along the Tunisia coast (mean intensities between 30 and 40 cm/s), the meandering AIS (speeds between 12 and 25 cm/s) and two mesoscale permanent features (the cyclonic Medina Gyre - MG, and the anticyclonic Maltese Channel Crest - MCC) show similar patterns and intensities in all panels of Fig. 2. In the southern Ionian a permanent anticyclonic circulation is observed off the Libyan coast (between 15° and 19°E and 32–35°N). This structure, already detected by Menna and Poulain, 2010 and Poulain et al. (2012) and defined in Pinardi et al. (2015) as the Sirte Gyre (SG), shows an interannual variability in terms of intensities and shape but it is not influenced by the decadal reversal of NIG. Larger velocities (10–15 cm/s) are observed in the westward branch of the SG, located along the Libyan coast.

East of 15°E, anticyclonic (cyclonic) periods are characterised by the strengthening (weakening) of currents in the NIG and the weakening (strengthening) in the MIJ (Fig. 2 right panels). The NIG shape changed during the two different modes: throughout the anticyclonic mode, it is located between 17°E and 20°E and it was surrounded by cyclonic mesoscale structures along its western and eastern sides (Figs. 2a, 2b, 2e, 2f). During the cyclonic mode, the basin wide cyclonic circulation convoluted the mesoscale structures located along the coasts, therefore the cyclonic meander involved all the circulation structures of the northern Ionian (Figs. 2c, 2d, 2g, 2h). The anticyclonic NIG reached the largest mean geostrophic velocities (12–18 cm/s) at its northernmost portion (~ 39°N; Figs. 2b and 2f). The cyclonic NIG shows the largest velocities (10–12 cm/s) off the Gulf of Taranto and along the Calabrian coast (Figs. 2d and 2h).

The MIJ also changed its characteristics according to the NIG circulation modes: it appears as an intense (10–20 cm/s) south-eastward continuous currents that joined the SC and the CP during the cyclonic NIG (Figs. 2c and 2g), whereas it was generally less intense (less than 10 cm/s) and more fragmented during the anticyclonic NIG (Figs. 2a and 2e).

The PG shows a prominent interannual variability: this anticyclonic structure disappeared during the period 1993–1996 (Figs. 2a, 2b), and showed largest intensities during 2006–2010 (as large as 25 cm/s), and moderate speeds (15 cm/s) during the other two periods.

A quantitative comparison between the currents derived from drifter (Fig. 2, left panels) and satellite (Fig. 2, right panels) is out of the scope of this paper. However, it is important to note that quantitative discrepancies between the two data sets are imputable to (i) the wind-driven and ageostrophic currents included in the drifter velocity measurement (Poulain et al., 2012), (ii) the spatial and temporal gaps due to the non-uniform drifter density (Poulain et al., 2012), (iii) the spatial smoothing applied to the satellite altimetry data (Pujol and Larnicol, 2005).

During the anticyclonic period 2006–2010 (Figs. 2e, 2f) the northward extension of the NIG and its speeds were reduced with respect to the period 1993–1997 (Figs. 2a, 2b). The differences in intensities between the two periods can be explained in terms of the massive inflow of the Aegean dense water associated with the EMT. During the 1990s, due to a yet not completely understood chain of atmospheric, oceanic and hydrological interactions, the region of the Eastern Mediterranean Deep Water formation switched from the southern Adriatic to the

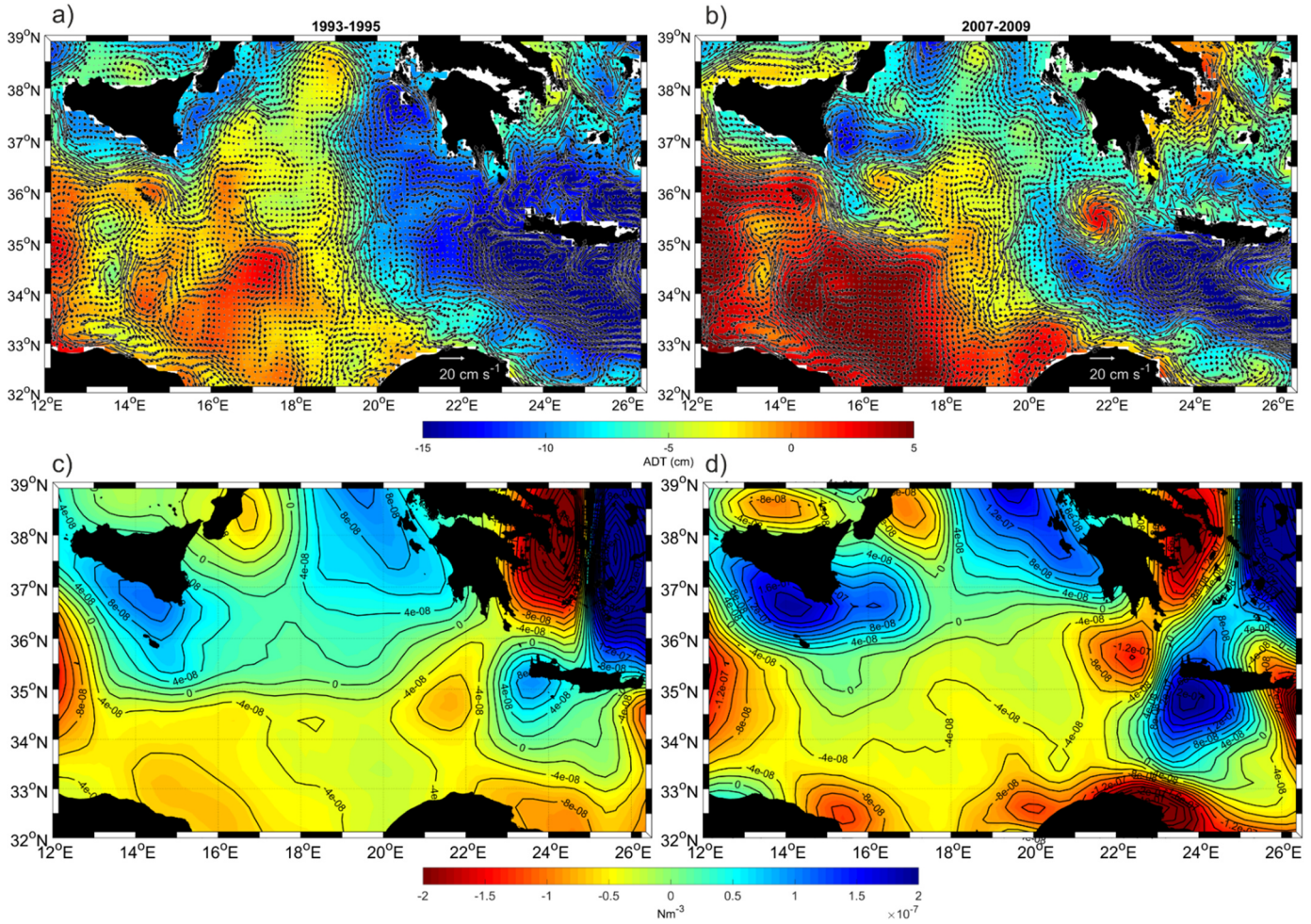

Fig. 3. Surface geostrophic currents (arrows) and absolute dynamic topography (colours) in the CMS during a) 1993–1995 and b) 2007–2009; wind stress curl during c) 1993–1995 and d) 2007–2009.

Cretan Sea (Roether et al., 2007). The production rate of the Eastern Mediterranean Deep Water of Aegean origin during the years of stronger formation (1992–1994) was an order of magnitude larger (2.8 Sv on average according Roether et al., 2007; 1.5 Sv according to Klein et al., 1999) than the rate of Eastern Mediterranean Deep Water of Adriatic origin (0.3 Sv; Roether and Schlitzer, 1991; Gačić et al., 1996). This phenomenon, known as EMT, caused changes not only in the deep layers but also over the entire water column (Roether et al., 2007; Gačić et al., 2010). We can speculate that, due to the massive inflow of dense water during the EMT, the horizontal pressure gradients in the IS were larger with respect to a no-EMT situation, inducing a stronger currents in the period 1993–1996.

The difference in shape between the anticyclonic NIG of 1993–1996 (Figs. 2a, 2b) and that of 2006–2010 (Figs. 2e, 2f), on the other hand, can be associated with the interannual variability of the MRV. This mesoscale structure has often a meridionally elongated shape and it is squeezed along the eastern coast of Sicily (Fig. 3a; Fig. 2 in Sorgente et al., 2011). During the period 2007–2009 it assumed a zonal extension and partially obstructed the inflow of the AW in the northern Ionian (Fig. 3b). In Fig. 3 (upper panels), we compare the mean ADT and AGV in the three-year period characterised by the strengthening of the MRV (2007–2009) with a three-year period selected during the previous anticyclonic NIG mode (1993–1995). In 1993–1995 the AIS flows directly northward from the SC toward the northern Ionian, describing a strong meandering current parallel to the eastern Sicily and Calabrian coasts and strengthening the eastern branch of the MRV (Fig. 3a). In 2007–2009 the zonal-elongated MRV obstructed the inflow of AW in the northern Ionian (Fig. 3b). The AIS partially flowed southward feeding the MIJ, and partially flowed eastward moving along the edges of the MRV and feeding an anticyclonic meander around 37°N (Fig. 3b); the eastward deflection of the ASI along the southern branch of the zonally – elongated MRV was clearly detected also by drifter mean currents in 2006–2010 (Fig. 2e). The flow towards the northern Ionian was strongly reduced, and, in any case, its path was conditioned by the presence of MRV. In order to explain the possible causes of the MRV strengthening in 2007–2009 we compare the AGV and ADT fields with the corresponding maps of the mean wind - stress vorticity (Figs. 3c and 3d). Even if geostrophic currents are not directly influenced by wind, the sea surface height is still linked to the underlying density field in the upper layer, which in turn is influenced by the wind-induced divergence (via Ekman pumping). The wind – stress vorticity field in 1993–1995 was generally weaker than in 2007–2009. The strength, the shape and the location of the mesoscale and sub-basin scale eddies appear influenced by the wind vorticity field. In particular, during 2007–2009 the zonally elongated shape of the MRV (Fig. 3b) resembled the pattern of the wind vorticity along the eastern coast of Sicily (Fig. 3d). The relation between the wind input and the MRV was also suggested in Lermusiaux and Robinson (2001).

Another mesoscale feature controlled by the wind-stress curl is the PG, (Ayoub et al., 1998; Mkhinini et al., 2014). The wind vorticity behaviour with time however was anticyclonic throughout the study period confirming that the PG is forced by the wind-stress curl. It was present at the eastern shore of the IS most of the time (Fig. 2) except in the period 1993–1995 when all the PG area was characterised by a

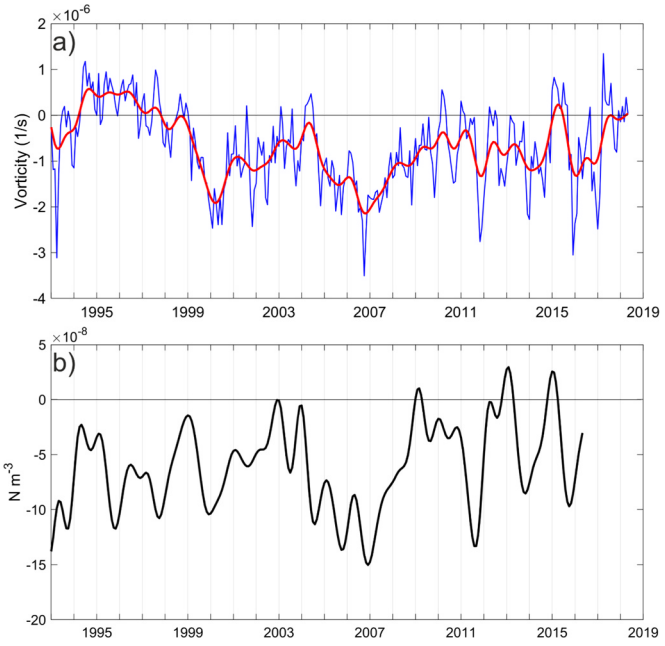

Fig. 4. a) Time series of the monthly, spatially averaged current vorticity (blue line) and low-pass filtered (13 months) current vorticity (red line) in the Pelops Gyre; b) time series of the monthly, spatially averaged low-pass filtered (13 months) wind-stress vorticity.

weak cyclonic vorticity (Fig. 3a). Then the current vorticity was always negative in the successive years (Fig. 4a). The interannual variability of the PG, that emerged in Figs. 2 and 3, was investigated by looking at the time series of the wind and current vorticities, spatially averaged in the area where this gyre persists (Fig. 4; geographical references defined in Section 2). The PG area shows a positive (cyclonic) circulation during the period 1994–1997, whereas in the rest of the study period the current vorticity was negative (Fig. 4a). The wind stress curl in the region of PG was predominantly negative all the time producing an anticyclonic vorticity input; positive values were observed only in some months of 2009, 2013 and 2015 but were too weak and isolated to be responsible of a circulation reversal. From these considerations, we conclude that the anomalous behaviour of PG during 1994–1997 was caused by internal forcing. The period of absence of PG i.e. of the prevalence of the cyclonic vorticity in the PG area coincided with the EMT period. This feature can be explained in terms of the forcing by the dense water plume coming from the Aegean Sea. As shown by laboratory and numerical experiments (Spall and Price, 1998; Etling et al., 2000; Lane-Serff and Baines, 2000), the dense water plume induces cyclonic vortices in the upper layer, which then move along the coast to the right-hand side of the outflow looking seaward. This way the input of the cyclonic vorticity generated by the dense water plume overwhelmed the wind input in the PG area. When the Adriatic became again the primary source of the dense water and the Aegean presumably stopped to produce a dense water, the area of the cyclonic vorticity moved along the western IS coast, while the PG became very prominent depending only on the wind curl input.

In order to describe in more details the basin-wide flow and its possible interaction with the mesoscale quasi-permanent features, we performed a more detailed analysis on some indicators of the large-scale circulation. Firstly, surface salinity fields confirm the enhanced flow of the AW in the northern Ionian during the anticyclonic phases of the NIG (low salinity values; Figs. 5a and 5c) and its reduction during the cyclonic phases, that facilitated the inflow of surface waters of Levantine origin (high salinity values; Figs. 5b, 5d). Salinity fields captured also the response of the AW flow to the zonal elongated MRV occurred in 2007–2009; the inflow of the less saline AW in the northern Ionian was weaken during the period 2006–2010 (Fig. 5c) with respect to the previous anticyclonic phase (Fig. 5a), and the AW was mainly trapped south of 37°N (Fig. 5c).

The interannual 'deseasonalised' EKE spatial distribution (Fig. 6) emphasizes the areas of the CMS where there are larger or smaller interannual variabilities of the surface currents. Larger values (as large as 80–100 cm^2 s^{-2}) in the southern part of CMS (south of 36°S), in particular in the SC (MCC), in the southern Ionian (MIJ pathway and SG), in the CP and in the PG signature. In the northern Ionian the levels of EKE were modest (30–50 cm^2 s^{-2}), associated with the decadal NIG reversals.

In order to study in more details the behaviour of the circulation in the geographical area characterised by decadal variations in the CMS, we calculated the time series of the surface geostrophic velocities through five transects. Transect locations (and orientation) represent a compromise between the need to intercept the main pathways of surface currents in the CMS (suitable for all the circulation modes that can occur in the basin), and the need to sample the most interesting areas from a dynamical point of view (local maxima of the EKE interannual variability). The transects selected, from west to east (Fig. 6), are positioned: 1) along the Tunisia coast (Tunisia transect) to intercept the flow of AW upstream of the SC; 2) in the SC (SC transect) to observe the variability of the AIS; 3) in the southern Ionian (southern Ionian transect) and 4) northern Ionian (northern Ionian transect) to describe the behaviour of the MIJ and of the NIG, respectively; 5) at the entrance of the CP (CP transect) to intercept the inflow of surface water in the Levantine Basin.

Time series of the mean surface geostrophic velocities (normal component), that cross the transects depicted in Fig. 6, are shown in Fig. 7. A prominent interannual variability dominated the transport across the Tunisia and SC transects (Fig. 7), whereas decadal variations prevailed to the East of SC (Fig. 7). The southern Ionian transect (Fig. 7) intercepts the flux of MIJ showing a decadal oscillation in phase with the CP transect (Fig. 7), and perfectly out-of-phase with the northern Ionian transect (Fig. 7). Part of the AW was carried toward the northern Ionian from the AIS during the anticyclonic NIG, before crossing the southern Ionian transect, producing a reduced geostrophic flux through the southern Ionian and CP transects and an increased (positive/eastward) flux through the northern Ionian transect. Cyclonic phases of the NIG blocked the inflow of the AW in the northern Ionian leading to a larger geostrophic flux toward the southern Ionian and CP transects and a negative (westward) current toward the northern Ionian transect.

The time series of geostrophic fluxes across the CP transect (Fig. 7) shows the interannual variability superimposed to the decadal one. Interannual variations can be ascribed to the pronounced mesoscale activity observed at the southern entrance of the CP transect (related to the instability of the coastal current; see Fig. 6) and/or east of the Sicily (interannual variability of the MRV). Two anomalous behaviours are observed in the time series. The first one occurred in 2007–2009, when the flux increased despite the anticyclonic circulation of the NIG, probably due to the strengthening of the MRV and its zonally elongated shape near the eastern Sicily coast (see Figs. 2e, 2f and 3b) as already indicated by Bessieres et al. (2013). The MRV shape (Fig. 3b) obstructed the inflow of AW in the northern Ionian (Fig. 5c) inducing a cyclonic-like event, characterised in Fig. 7 by an increase of the geostrophic fluxes at the SIT and CP transects. The time series of an indicator defined by Bessieres et al. (2013) displays positive/negative values during the anticyclonic/cyclonic phases, respectively (Figure 16 of Bessieres et al., 2013). During the period 2006–2010 their indicator shows positive values (anticyclonic condition), except in 2007 when it shows a negative peak (cyclonic-like conditions). Bessieres et al. (2013) concluded that the period 2006–2010 was a transitional state (defined as "anticyclonic-zonal") between the cyclonic modes occurred before 2006 and after 2010; in this period, the anticyclonic NIG was concurrent with a strong MIJ (Figs. 2e, 2f, 3b). From the results of the present work, however we sustain that there was no transition state in 2006–2010, but an anticyclonic phase characterised by the presence of

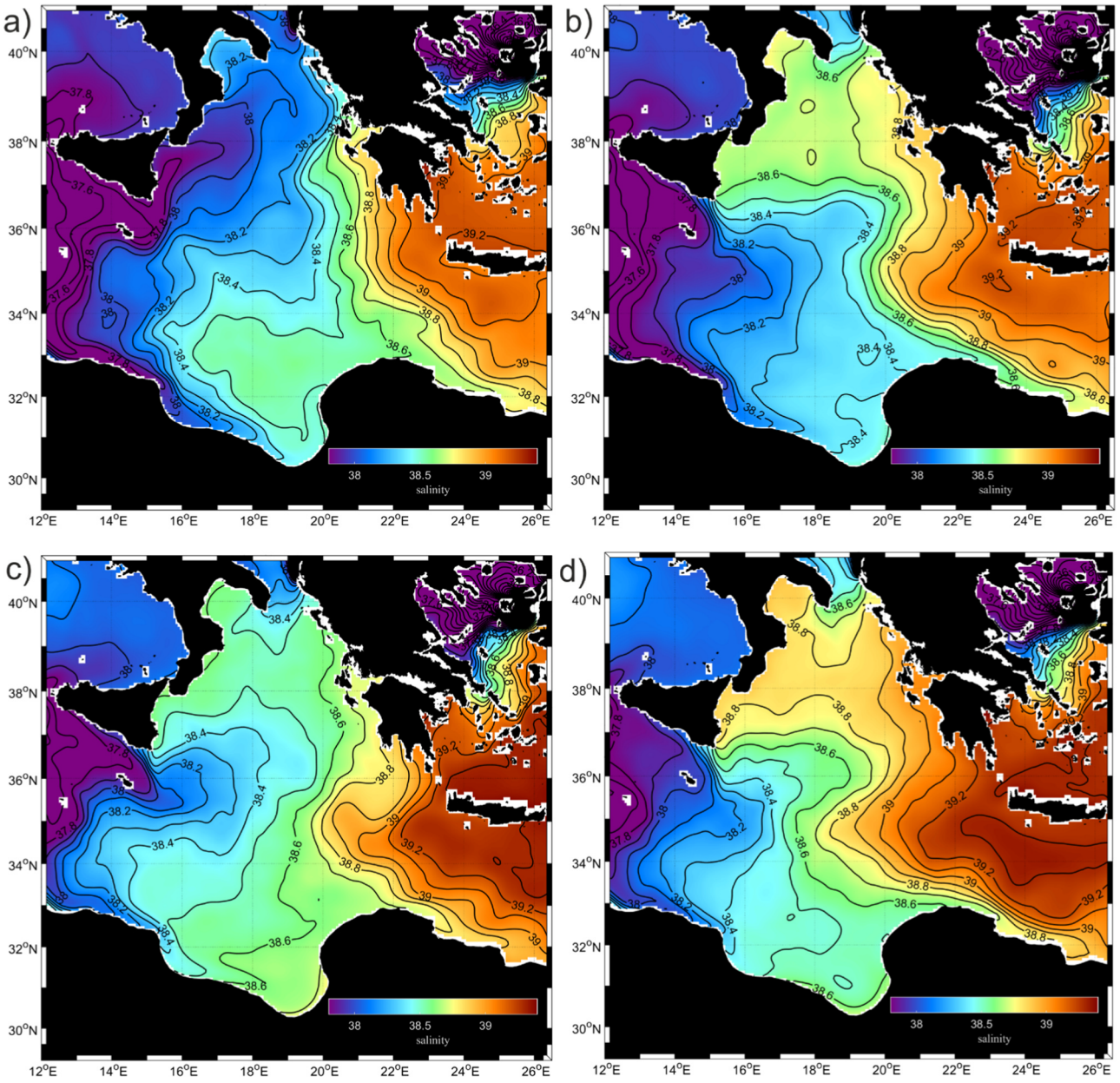

Fig. 5. Surface salinity patterns in the CMS for the periods a) 1993–1996, b) 1997–2005, c) 2006–2010, d) 2011–2015.

the strong MRV along the Italian coasts of the northern Ionian, which blocked the northward flow of the AIS and induced a cyclonic-like events in the MIJ and CP.

The second anomaly in the geostrophic velocity time series of the CP transect was observed in 2012–2013 (Fig. 7), when it probably responded to the premature and transient inversion of the NIG from cyclonic to anticyclonic, related to the extremely strong winter 2012 in the Adriatic (Gacic et al., 2014) leading to a strong weakening of the transport at CP transect and positive values in the time series of the northern Ionian transect (Fig. 7) between mid-2012 and the first months of 2013.

4. Conclusions

The CMS represents a crossroad of all waters participating to the zonal overturning circulation and it is the main storage of dense water formed in the Eastern Mediterranean. The upper layer of the CMS is a complex dynamical system closely linked to the interaction among internal and external forcing varying on interannual and quasi-decadal time-scales.

The quasi-decadal reversals of the surface circulation in the northern Ionian influences the shape and the intensities of the basin-scale circulation structures (NIG, MIJ). On the other hand, the interannual variability, mainly driven by the sudden and/or extreme climatic events and by the wind stress curl, influences the quasi-permanent mesoscale structures (PG and MRV).

The interannual variability of quasi-permanent mesoscale structures produces some differences in the basin-wide circulation within the same quasi-decadal circulation mode. The anticyclonic mode 2006–2010 differed from the previous one 1993–1996 in that it was characterised by the zonally elongated shape of the MRV, on the western side of the northern Ionian, and by the strengthening of the PG, on the eastern side of the northern Ionian. These quasi-permanent mesoscale structures are driven by the wind-curl but according our results it is shown that they are also influenced by internal forcing. The MRV was squeezed against the eastern coast of Sicily during the EMT

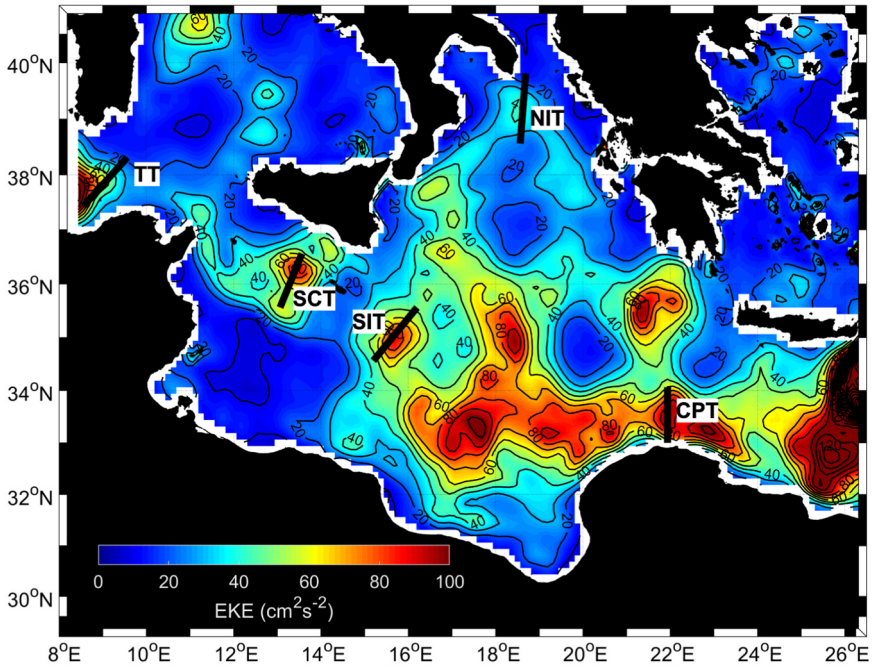

Fig. 6. Eddy kinetic energy in the CMS associated with the interannual variability of the current field; black segments denote the location of transects used in Fig. 7. Acronyms: Tunisia Transect (TT), Southern Sicily Transect (SCT), Southern Ionian Transect (SIT); Northern Ionian Transect (NIT), Cretan Passage Transect (CPT).

(1993–1996; Figs. 2a, 2b, 3a), when the Eastern Mediterranean Deep Water in the IS was of Aegean origin ("Aegean" anticyclonic mode), whereas it showed a zonally elongated shape in 2006–2010 (Figs. 2e, 2f, 3b), when the Eastern Mediterranean Deep Water was of Adriatic origin ("Adriatic" anticyclonic mode). Its zonally elongated shape contrasted the northward path of the AIS and reduced the AW flow northward (Fig. 3b).

The PG disappeared during the "Aegean" anticyclonic mode (Figs. 2a and 2b) even though the wind curl input was anticyclonic; on the other hand, it reached its maximum intensity during the "Adriatic" anticyclonic mode (Figs. 2e and 2f). The explanation for the PG behaviour is once again linked to the location of the dense-water formation

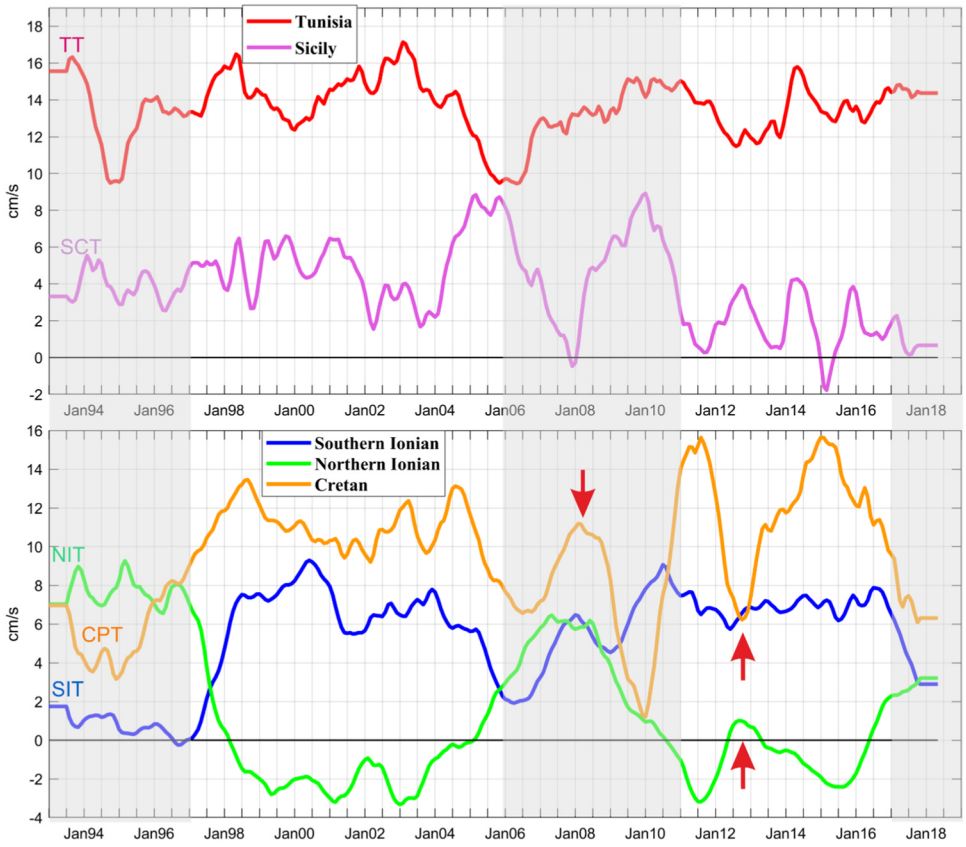

Fig. 7. Time series of mean geostrophic currents (13-months moving average) across transects showed in Fig. 6. Anticyclonic periods are emphasized in light grey. Red arrows point out the periods with anomalous behaviours of the CMS. Acronyms: Tunisia Transect (TT), Southern Sicily Transect (SCT), Southern Ionian Transect (SIT); Northern Ionian Transect (NIT), Cretan Passage Transect (CPT).

site. During the "Aegean" anticyclonic mode (1993–1996), the IS deepest layer was filled by dense water of Aegean origin, the Cretan Sea Outflow Water (CSOW), spreading from the Cretan Passage and invading the eastern Ionian northwards along a cyclonic path (Roether et al., 1996, 2007). The ADT maps in Figs. 2a and 3a denote a presence of strong cyclonic mesoscale activity at the surface along the CSOW dense water path, on the eastern flank of the Ionian (Bensi et al., 2013; Amiati et al., 2016), that overwhelmed the anticyclonic wind forcing, and led to the disappearance of the PG. After the year 2000, Adriatic resumed its role as main dense water source for the Eastern Mediterranean (Klein et al., 1999), so the western Ionian slope was again occupied by the Adriatic Dense Water spreading toward the Ionian abyssal plain and moving southward along the western Ionian flank (Bensi et al., 2013). For this reason, during the "Adriatic" anticyclonic mode (2006–2010), the cyclonic mesoscale activity was mainly concentrated along the western Ionian slope, whilst the PG was again prominent. Our conclusion is that the disappearance of the PG was due to the massive spreading of the CSOW in the Ionian Sea. This interpretation is supported by the laboratory studies by Etling et al. (2000) which showed the occurrence of mesoscale cyclonic eddies in the upper layer along the path of dense water outflow at bottom. Further support to our interpretation can be found in the experimental results presented by Lane-Serff and Baines (1999): The propagation of dense water characterised by the formation of domes gives birth to cyclonic vortices in the upper water layer, the dominant generation mechanism consisting in an adjustment of the potential vorticity in the outflowing layer to the lower potential vorticity of the upper layer environment. As a result, the stretching of the water column induces the formation of strong, mesoscale cyclonic eddies. In this process, the presence of an active intermediate layer may enhance the resulting vortex intensity (Spall and Price, 1998).

During the cyclonic modes, the MRV was incorporated in the large basin-wide cyclonic gyre and the PG was present and prominent, as well as during the "Adriatic" anticyclonic mode, since it is mainly determined by the wind stress curl input (Figs. 2c, 2d, 2g, 2h).

The cyclonic mode of 2011–2016 also differed from the previous one (1997–2005) because it was temporarily interrupted by the forcing of the climatic event which involved the entire Adriatic Sea. More specifically, the winter of 2012 was extremely severe in the northern (Bensi et al., 2013; Mihanović et al., 2013) and southern (Gačić et al., 2014) Adriatic, resulting in the formation of extremely dense Adriatic Dense Water. The spread of this water into the IS inverted the bottom pressure gradient and generate the temporary NIG reversal (Gačić et al., 2014). This reversal was a short-lived phenomena because of the limited amount of Adriatic Dense Water involved in the spreading and it was observed in the northern Ionian in the second half of 2012 (Fig. 7). The consequent transient reduction of the AW flux toward the Levantine Basin is reported in Fig. 7.

The present study highlights the sensitivity of CMS to the mesoscale variability and climatic forcing. The interannual variability of the quasi-permanent mesoscale structures, induced by internal and external forcing, and climatic shifts, like the one occurred during the EMT, can change substantially the basin-wide circulation and the water mass dispersion. These changes affect the characteristic of the NIG reversals cycle and their periodicity. In this sense, the NIG reversal can be seen as a gauge of the Mediterranean variability, and its behaviour can be usefully interpreted as a signal of changes in circulation and/or water masses distribution in the basin.

References

Artale, V., Calmante, S., Malanotte-Rizzoli, P., Pisacane, G., Rupolo, V., Tsimplis, M., 2006. The Atlantic and Mediterranean Sea as connected systems. In: Lionello, P., Malanotte-Rizzoli, P., Boscoli, R. (Eds.), Mediterranean Climate Variability. vol. 4. Elsevier, Amsterdam, pp. 283–323.

Atlas, R., Hoffman, R.N., Ardizzone, J., Leidner, S.M., Jusem, J.C., Smith, D.K., Gombos, D., 2011. A cross-calibrated, multiplatform ocean surface wind velocity product for meteorological and oceanographic applications. Bull. Am. Meteorol. Soc. 92, 157–174. https://doi.org/10.1175/2010BAMS2946.1.

Ayoub, N., Le Traon, P.Y., De Mey, P., 1998. A description of the Mediterranean surface variable circulation from combined ERS-1 and TOPEX/POSEIDON altimetric data. J. Mar. Syst. 18 (1–3), 3–40. https://doi.org/10.1016/S0924-7963(98)80004-3.

Bensi, M., Cardin, V., Rubino, A., Notarstefano, G., Poulain, P.M., 2013. Effects of winter convection on the deep layer of the Southern Adriatic Sea in 2012. J. Geophys. Res.-Oceans 118, 6064–6075. https://doi.org/10.1002/2013JC009432.

Bessieres, L., Rio, M.H., Dufau, C., Boone, C., Pujol, M.I., 2013. Ocean state indicators from MyOcean altimeter products. Ocean Sci. 9, 545–560. https://doi.org/10.5194/os-9-545-2013.

Borzelli, G.L.E., Gačić, M., Cardin, V., Civitarese, G., 2009. Eastern Mediterranean Transient and reversal of the Ionian Sea circulation. Geophys. Res. Lett. 36, L15108. https://doi.org/10.1029/2009GL039261.

Brandt, P., Rubino, A., Quadfasel, D., Alpers, W., Sellschopp, J., Fiekas, H.V., 1999. Evidence for the influence of Atlantic-Ionian Stream fluctuations on the tidally induced internal dynamics in the Strait of Messina. J. Phys. Oceanogr. 29, 1071–1080.

Cardin, V., Civitarese, G., Hainbucher, D., Bensi, M., Rubino, A., 2015. Thermohaline properties in the Eastern Mediterranean in the last three decades: Is the basin returning in the pre-EMT situation? Ocean Sci. 11 (1), 53–66.

Civitarese, G., Gačić, M., Eusebi Borzelli, G.L., Lipizer, M., 2010. On the impact of the bimodal oscillating system (BiOS) on the biogeochemistry and biology of the Adriatic and Ionian Seas (eastern Mediterranean). Biogeosciences 7, 3987–3997. https://doi.org/10.5194/bg-7-3987-2010.

Demirov, E., Pinardi, N., 2002. Simulation of the Mediterranean Sea circulation from 1979 to 1993: Part I. The interannual variability. J. Mar. Syst. 33–34, 23–50. https://doi.org/10.1016/S0924-7963(02)00051-9.

Etling, D., Gelhardt, F., Schrader, U., Brennecke, F., Kühn, G., Chabert d'Hieres, Didelle, H., 2000. Experiments with density currents on a sloping bottom in a rotating fluid. Dyn. Atmos. Oceans 31, 139–164.

Gačić, M., Borzelli, G.L.E., Civitarese, G., Cardin, V., Yari, S., 2010. Can internal processes sustain reversals of the ocean upper circulation? The Ionian Sea example. Geophys. Res. Lett. 37, L09608. https://doi.org/10.1029/2010GL043216.

Gačić, M., Civitarese, G., Borzelli, G.L.E., Kovacevic, V., Poulain, P.-M., Theocharis, A., Menna, M., Catucci, A., Zarokanellos, N., 2011. On the relationship between the decadal oscillations of the Northern Ionian Sea and the salinity distributions in the Eastern Mediterranean. J. Geophys. Res. 116, C12002. https://doi.org/10.1029/2011JC007280.

Gačić, M., Civitarese, G., Kovacevic, V., Ursella, L., Bensi, M., Menna, M., Cardin, V., Poulain, P.-M., Cosoli, S., Notarstefano, G., Pizzi, C., 2014. Extreme winter 2012 in the Adriatic: an example of climatic effect on the BiOS rhythm. Ocean Sci. 10, 513–522. https://doi.org/10.5194/os-10-513-2014.

Gačić, M., Kovacevic, V., Manca, B.B., Papageorgiou, E., Poulain, P.-M., Scarazzato, P., Vetrano, A., 1996. Thermohaline properties and circulation in the Strait of Otranto. In: Briand, F. (Ed.), Dynamic of Mediterranean Straits and Channels. vol. 2. pp. 117–145.

Gačić, M., Schroeder, K., Civitarese, G., Cosoli, S., Vetrano, A., Borzelli, G.L.E., 2013. Salinity in the Sicily channel corroborates the role of the Adriatic-Ionian bimodal oscillating system (BiOS) in shaping the decadal variability of the Mediterranean overturning circulation. Ocean Sci. 9, 83–90. https://doi.org/10.5194/os-9-83-2013.

Klein, B., Roether, W., Manca, B.B., Bregant, D., Beitzel, V., Kovačević, V., Lucchetta, A., 1999. The large deep water transient in the eastern Mediterranean. Deep Sea Res. Part I 46, 371–414. https://doi.org/10.1016/S0967-0637(98)00075-2.

Lane-Serff, G., Baines, P.G., 2000. Eddy formation by overflows in stratified water. J. Phys. Oceanogr. 30, 327–337.

Lavigne, H., Civitarese, G., Gačić, M., D'Ortenzio, F., 2018. Impact of the decadal reversals of the North Ionian circulation on phytoplankton phenology. Biogeosciences 15, 4431–4445. https://doi.org/10.5194/bg-15-4431-2018.

Lermusiaux, P.F.J., Robinson, A.R., 2001. Features of dominant mesoscale variability, circulation patterns and dynamics in the Strait of Sicily. Deep-Sea Res. I 48, 1953–1997.

Malanotte-Rizzoli, P., Manca, B.B., Ribera D'Alcalà, M., Theocharis, A., Bergamasco, A., Bregant, D., Budillon, G., Civitarese, G., Georgopulos, D., Michelat, A., Sansone, E., Scarazzato, P., Souvermezoglou, E., 1997. A synthesis of the Ionian Sea hydrography, circulation and water masses pathways during POEM-Phase I. Prog. Oceanogr. 39, 153–204.

Menna, M.R., Gerin, A. Bussani, P.-M., 2018. Poulain: Surface currents and temperature data db_med24_nc_1986_2016_kri05 - db_med24_nc_1986_2016_kri6hF. ⟨http://dx.doi.org/10.6092/7a8499bc-c5ee-472c-b8b5-03523d1e73e9⟩.

Menna, M., Gerin, R., Bussani, A., Poulain, P.-M., 2017. The OGS Mediterranean drifter database: 1986–2016. Technical report 2017/92 Sez. OCE 28 MAOS.

Menna, M., Poulain, P.-M., 2010. Mediterranean intermediate circulation estimated from Argo data in 2003–2010. Ocean Sci. 6, 331–343. https://doi.org/10.5194/os-6-331-2010.

Mihanović, H., Vilibić, I., Carniel, S., Tudor, M., Russo, A., Bergamasco, A., Bubić, N., Ljubešić, Z., Viličić, D., Boldrin, A., Malačič, V., Celio, M., Comici, C., Raicich, F., 2013. Exceptional dense water formation on the Adriatic shelf in the winter of 2012. Ocean Sci. 9, 561–572. https://doi.org/10.5194/os-9-561-2013.

Mkhinini, N., Coimbra, A.L.S., Steger, A., Arsouze, T., Taupier-Letage, I., Beranger, K., 2014. Long-lived mesoscale eddies in the eastern Mediterranean Sea: analysis of 20 years of AVISO geostrophic velocities. J. Geophys. Res. Oceans 119, 8603–8626. https://doi.org/10.1002/2014JC010176.

Notarstefano, G., Menna, M., Legeais, J.-F., et al., 2019. Reversal of the Northern Ionian circulation in 2017, section 4.5 in Von Schuckmann et al. Copernicus Marine Service Ocean State Report. J. Oper. Oceanogr (under final review).

Ozer, T., Gertman, I., Kress, N., Silverman, J., Herut, B., 2017. Interannual thermohaline

(1979–2014) and nutrient (2002–2014) dynamics in the Levantine surface and intermediate water masses, SE Mediterranean Sea. Glob. Planet. Change 151, 60–67. https://doi.org/10.1016/j.gloplacha.2016.04.001.

Pinardi, N., Zavatarelli, M., Adani, M., Coppini, G., Fratianni, C., Oddo, P., Simoncelli, S., Tonani, M., Lyubartsev, V., Dobricic, S., Bonaduce, A., 2015. Mediterranean Sea large-scale low-frequency ocean variability and water mass formation rates from 1987 to 2007: a retrospective analysis (ISSN 0079-6611). Prog. Oceanogr. 132, 318–332. https://doi.org/10.1016/j.pocean.2013.11.003.

Pisacane, G., Artale, V., Calmanti, S., Rupolo, V., 2006. Decadal oscillations in the Mediterranean Sea: a result of the overturning circulation variability in the eastern basin, 31, pp. 257–271.

Poulain, P.-M., Menna, M., Mauri, E., 2012. Surface geostrophic circulation of the Mediterranean Sea derived from drifter and satellite altimeter data. J. Phys. Oceanogr. 42 (6), 973–990. https://doi.org/10.1175/JPO-D-11-0159.1.

Pujol, M.-I., Larnicol, G., 2005. Mediterranean Sea eddy kinetic energy variability from 11 years of altimetric data. J. Mar. Syst. 58 (4), 121–142. https://doi.org/10.1016/j.jmarsys.2005.07.005.

Reale, M., Salon, S., Crise, A., Farneti, R., Mosetti, R., Sannino, G., 2017. Unexpected covariant behaviour of the Aegean and Ionian seas in the period 1987–2008 by means of a nondimensional sea surface height index. J. Geophys. Res. Ocean. 122, 8020–8033. https://doi.org/10.1002/2017JC012983.

Robinson, A.R., Leslie, W.G., Theocharis, A., Lascaratos, A., 2001. Mediterranean Sea Circulation, Encyclopedia of Ocean Science. Academic Press, pp. 1689–1706. https://doi.org/10.1006/rwos.2001.0376.

Roether, W., Klein, B., Manca, B.B., Theocharis, A., Kioroglou, S., 2007. Transient Eastern Mediterranean deep waters in response to the massive dense-water output of the Aegean Sea in the 1990s. Prog. Oceanogr. 74, 540–571. https://doi.org/10.1016/j.pocean.2007.03.001.

Roether, W., Manca, B.B., Klein, B., Bregant, D., Georgopoulos, D., Beitzel, V., Kovaćevič, V., Luchetta, A., 1996. Recent changes in Eastern Mediterranean deep waters. Science 271, 333–335. https://doi.org/10.1126/science.271.5247.333.

Roether, W., Schlitzer, R., 1991. Eastern Mediterranean deep-water renewal on the basis of chlorofluoromethane and tritium data. Dyn. Atmos. Oceans 15, 333–354. https://doi.org/10.1016/0377- 0265(91)90025-B.

Schroeder, K., Chiggiato, J., Bryden, H.L., Borghini, M., Ben Ismail, S., 2016. Abrupt climate shift in the Western Mediterrnaean Sea. Sci. Rep. 6, 23009. https://doi.org/10.1038/srep23009.

Shabrang, L., Menna, M., Pizzi, C., Lavigne, H., Civitarese, G., Gačić, M., 2016. Long-term variability of the southern Adriatic circulation in relation to North Atlantic Oscillation. Ocean Sci. 12 (1), 233–241. https://doi.org/10.5194/os-12-233-2016.

Simoncelli, S., Fratianni, C., Pinardi, N., Grandi, A., Drudi, M., Oddo, P., Dobricic, S., 2014. Mediterranean Sea physical reanalysis (MEDREA 1987–2015) (version 1). Copernic. Monit. Environ. Mar. Serv. (CMEMS). https://doi.org/10.25423/medsea_reanalysis_phys_006_004.

Simoncelli, S., Pinardi, N., Fratianni, C., Dubois, C., Notarstefano, G., 2018. Water mass formation processes in the Mediterranean Sea over the past 30 years. Copernicus marine environment monitoring service Ocean state report. J. Oper. Oceanogr. 11, S1–S142. https://doi.org/10.1080/1755876X.2018.1489208. (in von Schuckmann et al. 2018.

Sorgente, R., Olita, A., Oddo, P., Fazioli, L., Ribotti, A., 2011. Numerical simulation and decomposition of kinetic energy in the Central Mediterranean: insight on mesoscale circulation and energy conversion. Ocean Sci. 7, 503–519. https://doi.org/10.5194/os-7-503-2011.

Spall, M.A., Price, J.F., 1998. Mesoscale variability in Denmark Strait: the PV outflow hypothesis. J. Phys. Oceanogr. 28, 1598–1623.

Theocharis, A., Krokos, G., Velaoras, D., Korres, G., 2014. An internal mechanism driving the alternation of the Eastern Mediterranean dense/deep water sources. In: Borzelli, G.L.E. (Ed.), The Mediterranean Sea: Temporal Variability and Spatial Patterns. 202. pp. 113–137. https://doi.org/10.1002/9781118847572.ch8. (AGU Geophys. Monogr. Ser.).

Yelland, M., Taylor, P.K., 1996. Wind-stress measurements from the open ocean. J. Phys. Oceanogr. 26, 541–558.